Study of Experimental and Calculated Flame Speed of Methane/Oxygen-Enriched Flame in Gas Turbine Conditions As a Function of Water Dilution: Application to CO2 Capture by Membrane Processes

G. Cabot, J. Chica Cano, S. de Persis, Fabrice Foucher

Proceedings of ASME Turbo Expo 2017: Turbomachinery Technical Conference and Exposition
GT2017
June 26-30, 2017, Charlotte, NC, USA

GT2017-64111

STUDY OF EXPERIMENTAL AND CALCULATED FLAME SPEED OF METHANE/OXYGEN-ENRICHED FLAME IN GAS TURBINE CONDITIONS AS A FUNCTION OF WATER DILUTION. APPLICATION TO CO_2 CAPTURE BY MEMBRANE PROCESSES

G. Cabot, J.P. Chica Cano
CORIA UMR 6614
Normandie Université
Rouen, France

S. de Persis,
ICARE CNRS UPR 3021
Université Orléans
Orléans, France

F. Foucher
PRISME
Université Orléans,
Orléans, France

ABSTRACT

A solution for CCS (Carbon Dioxide Capture and Sequestration of CO_2) is oxycombustion. Due to the high cost of pure O_2 production, however, other approaches recently emerged such as post-combustion coupled with Oxygen Enhanced Air (OEA). This is the solution studied in this paper, which presents an innovative gas turbine cycle, the Oxygen Enriched Air Steam Injection Gas Turbine Cycle (OEASTIG). The OEASTIG cycle is composed of Methane combustion with OEA (Oxygen Enhanced Air), EGR (Exhaust Gas Recirculation) and H_2O coming from a STIG (Steam Injection Gas Turbine). CO_2 capture is achieved by a membrane separator. The final aim of this work is to predict NO and CO emissions in the gas turbine by experimental and numerical approaches. Before carrying out this study, the validation of a reaction mechanism is mandatory. Moreover, this new gas turbine cycle impacts on the combustion zone and it is therefore necessary to understand the consequences of H_2O and CO_2 dilution on combustion parameters. While a large number of papers deal with CO_2 dilution, only a few papers have investigated the impact of water dilution on methane combustion. A study of the influence of H_2O dilution on the combustion parameters by experimental and numerical approaches was therefore carried out and is reported in the present paper. The paper is divided in three parts: i) description of the innovative gas turbine (OEASTIG) cycle and determination of the reactive mixtures compatible with its operation; ii) validation of the reaction mechanism by comparing laminar methane flame velocity measurements performed in a stainless steel spherical combustion chamber with calculations carried out in a freely propagating flame using the Chemical Workbench v.4.1. Package in conjunction with the GRIMech3.0 reaction mechanism; iii) Extrapolation to gas turbine conditions by prediction of flame velocities and determination of the feasible conditions from a gas turbine point of view (flame stability). In particular, mixtures (composed of $CH_4/O_2/N_2/H_2O$ or CO_2) leading to the same adiabatic temperature were investigated. Lastly, the influence of oxygen enrichment and H_2O dilution (compared to CO_2 dilution) were investigated.

NOMENCLATURE

ASU	: Air Separator Unit
CCS	: Capture and Sequestration of CO_2
EGR	: Exhaust Gas Recirculation
HRSG	: Heat Recovery Steam Generator
MCSU	: Membrane CO_2 Separator Unit
OEA	: Oxygen Enriched Air
OEASTIG	: Oxygen Enriched Air STIG Cycle
STIG	: Steam Injection Gas Turbine
TIT	: Turbine Inlet Temperature
Ω	: $X_{O2}/(X_{O2}+X_{N2})$ ratio

INTRODUCTION

Carbon dioxide capture and storage (CCS) is expected to play a significant role in CO_2 emission mitigation. Its use is adapted to

centralized, high CO_2 emitters such as Power Plants, in which capture, transport and sequestration costs can be minimized.

The post combustion CO_2 capture process using a membrane separator is a promising candidate, but its efficiency becomes interesting only if the CO_2 concentration in the combustion process exhaust gases is higher than 30% [1][2]. The use of Oxygen Enriched Air (OEA) as oxidant is a way to enrich the CO_2 concentration in the exhaust gas. Due to the production cost of OEA [3][4], an excess of OEA is not recommended. Consequently, the classical method of cooling the combustion chamber and the turbine inlet by an additional oxidant flow cannot be used. In the oxycombustion process, cooling is generally achieved by dry exhaust gas recirculation (EGR) and more precisely by CO_2 dilution [5]. The effects of CO_2 dilution on combustion have been extensively studied in numerous papers [5][6] and a drawback has been highlighted: CO_2 dilution drastically increases CO pollutant emissions. Consequently, the study of an alternative combustion, using H_2O as diluting gas, is proposed in this paper for gas turbine conditions (Steam injection, SI). Coupling CO_2 capture by a membrane and OEA/EGR/SI combustion is a new process that needs to be carefully studied because OEA, EGR and SI (represented by H_2O dilution) drastically modify the combustion parameters (such as flame velocities) even if the fuel is methane. For manufacturers, it is essential to determine these combustion parameters when designing the combustion chamber because they determine flame instabilities, pollutant emissions and flame structure [6][7].

As mentioned above, a huge number of studies in the literature focus on understanding the effect of oxygen enrichment and/or CO_2 dilution on methane laminar premixed flames [9][10], [11][12]. However, only a small number of fundamental flame speed studies of methane with H_2O dilution have been reported. Measurements performed on conical flames were reported in [13][14] and on outwardly expanding flames in [15][16]. The effect of pressure on laminar methane/air flames diluted with water was studied for the first time, in 1971, by Babkin et al. [16]. Their experimental device consisted of a spherical bomb that enabled the pressure to be varied from 0.1 to 7.0 MPa. In their study, they concluded that, for a given water content, the barometric exponent in the dependence of the velocity-pressure ($S_U \sim P^n$) decreased as the pressure rose. They also found that a higher water content corresponded to a greater reduction in the exponent. In 2009, Mazas et al. [14] studied the effect of O_2 enrichment in steam diluted methane flames but only at atmospheric pressure. In their experiments, performed in an axisymmetric burner, the O_2 percentage in the oxidant was varied from Ω=0.21 (air) to 1.0 (oxycombustion), the equivalence ratio from 0.8 to 1.6, and the steam dilution (in terms of water mole fraction in the reactants) from 0 to 0.5. They observed that the laminar burning velocity decrease was quasi-linear with increasing steam molar fraction, especially for highly oxygen-enriched flames. In 2011, Galmiche et al. [15] compared the effects of different diluents (N_2, CO_2 and H_2O) on laminar burning velocity at atmospheric pressure. They showed that CO_2 dilution had a greater influence than H_2O dilution, due to its molar heat capacity. In 2013, Albin et al. [13] studied the effect of steam dilution on laminar and turbulent methane/air flames at atmospheric pressure and for two different burners: Bunsen and V-flames. They concluded that a methane–air flame in ultra-wet conditions could be more than three times slower than a dry flame. Nevertheless, the study of oxycombustion diluted by water and operating in pressurized conditions has not been investigated.

The ultimate aim of our work will be to simulate the mixture and flow characteristics of a gas turbine combustor with a detailed reaction mechanism. This gas turbine network will predict pollutant emissions (CO and NO) over the whole operating domain of gas turbines and will be compared with experimental measurements performed in a reference gas turbine flame configuration [4]. Before making this calculation, a preliminary study, consisting in the validation of the reaction mechanism (GRIMech 3.0) [17], was done. It was carried out using an experimental approach, based on the measurement of flame velocities, operating in medium conditions of pressure and temperature corresponding to the highest limits of the experimental set-up [15]. The interest of this preliminary study is twofold: it is not only mandatory to validate the reaction mechanism but it is also very interesting from a fundamental point of view as it completes the experimental database and enriches our knowledge of the effect of H_2O dilution and O_2 enrichment on CH_4 combustion, in particular in pressurized conditions.

The present paper is divided in three parts, as follows:

- 1st part: Determination of a realistic reactive mixture obtained in an OEASTIG gas turbine thermodynamic cycle.
- 2nd Part: validation of the reaction mechanism in conditions as close as possible to those of the gas turbine (P=0.5 MPa, T_0=473K). Measurements and calculations of laminar methane flame velocities were compared in a freely propagating flame using the GRIMech3.0 reaction mechanism [17] and Chemical Workbench (CWB) v.4.1. Package [18]. Measurements of flame velocities of $CH_4/O_2/N_2/H_2O$ mixtures from 0.1MPa to 0.5 MPa (the highest pressure limit of the experimental set-up) were carried out in a spherical combustion chamber coupled with Schlieren measurement. This setup has been extensively described elsewhere [15] and is briefly described in section 2.1. The experimental conditions were as follows. The inlet temperature was 473 K (the highest temperature that can be reached in the experimental set-up) and the equivalence ratio ϕ defined by the following equation, was fixed at 1:

$$\phi = \frac{\left(X_{CH_4}/X_{O_2}\right)_m}{\left(X_{CH_4}/X_{O_2}\right)_s} \quad \text{(Eq.1)}$$

All the experiments presented in this paper were conducted in stoichiometric conditions corresponding to $\left(\frac{X_{O_2}}{X_{CH_4}}\right)_m = 2$ and oxygen content in the mixture is defined by Ω [14].

$$\Omega = \frac{X_{O_2}}{X_{O_2}+X_{N_2}} \quad \text{(Eq. 2)}$$

Ω = 0.21 for air and Ω = 1 for pure O_2, i.e., for oxycombustion conditions.

-3rd Part: calculations of laminar flame velocities in gas turbine conditions as a function of Ω, for an inlet temperature of T_0=700K, a pressure of P=1.7MPa and two adiabatic flame temperatures (2073K and 2273K) in the reactive zone. The effect of CO_2 dilution is also compared to H_2O dilution in terms of CO and NO pollutants.

1) EXAMPLE OF A STIG GAS TURBINE THERMODYNAMIC CYCLE

1.1. Description of the cycle

In this section, an example of a STIG gas turbine thermodynamic cycle coupled to a CO_2 capture process involving combustion with a high H_2O dilution rate is described; it is called OEASTIG. The simulation of this cycle was performed thanks to the EES (Engineering Equation Solver) code [19] and the CO_2 capture efficiency was optimized by varying the OEA quality (Ω_{OEA}) at the inlet of the process. Due to the cost of OEA production, the excess of OEA versus stoichiometric conditions was close to 0 [4] and the calculation was made for an equivalence ratio of 1. In this case, as the steam flow produced by the Heat Recovery Steam Generator HRSG is not sufficient to obtain by dilution a turbine inlet temperature (TIT) consistent with the thermal properties of the turbine alloy (e.g. 1473K), further dilution by exhaust gas recirculation is necessary. This leads to a reactive mixture in the combustion chamber inlet composed of OEA, EGR and Steam. One of the interests of this cycle is to produce dried exhaust gases with a high enough CO_2 concentration (greater than 30%) to enable CO_2 capture with a membrane process [20]. Details of the CO_2 capture process and the EES optimization can be found in [1][19]. Optimization of the CO_2 capture efficiency was achieved by fixing certain parameters in the different parts of the process and by varying only the Ω_{OEA}. The other parameters, such as the reactive mixture in the combustion chamber, were constrained. The power plant cycle shown in fig1 is a STIG cycle in which OEA is the oxidant. In the gas turbine module shown in figure 1, the equivalence ratio (1), the TIT (1473K), the pressure ratio (17:1), the combustion chamber pressure drop (5%) [21], the isentropic efficiencies of compressor and turbine (0.88)[22] were kept constant. In the HRSG, the pinch-point was 10 K and the superheated steam temperature was maintained 50 K lower than the temperature of exhaust gases from the gas turbine with a maximum value of 873K. In the CO_2 Capture Separation Unit, CO_2 capture rate, CO_2 quality and Membrane selectivity were maintained respectively at R = 0.9, $X_{CO2\ out}$ = 0.9 and α = 100 [1]. The OEA production cost was estimated from the work of Götlicher [3] assuming a cryogenic Air Separation Unit (ASU). At the exit of the HRSG, the exhaust gases were cooled in order to decrease EGR compression and to dry the EGR. The resulting water liquid flow is fed into the HRSG to produce Steam.

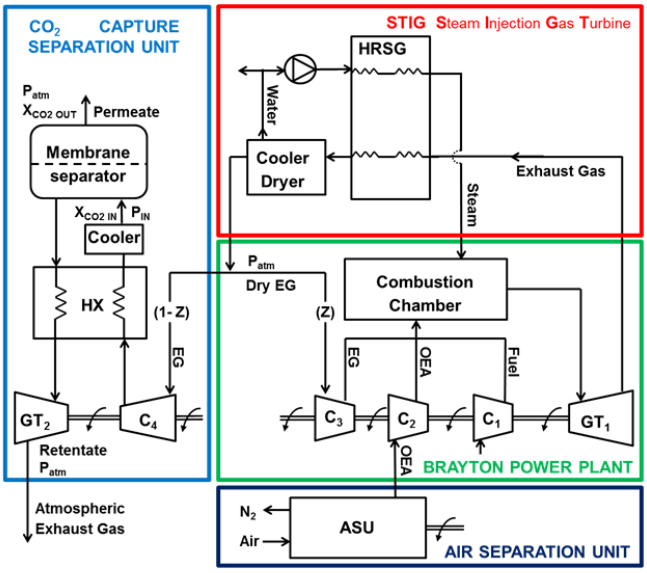

Figure 1: Scheme of the CO_2 capture hybrid process.

1.2. Capture efficiency

The capture efficiency was evaluated as previously described in [1][20][23]. The effect of CO_2 capture on the cycle thermal efficiency is presented in Figure 2.

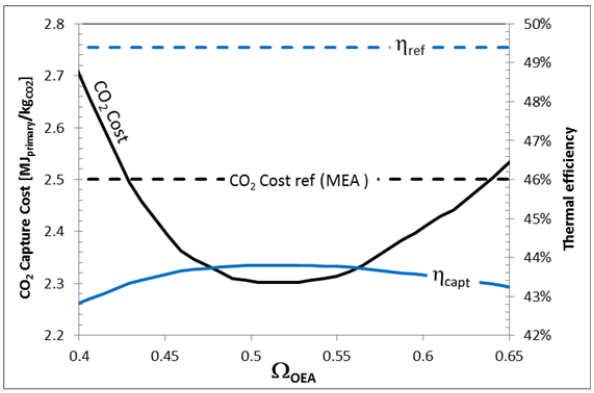

Figure 2: Evolution of the CO_2 capture cost (left-hand side scale, in black) and the thermal efficiency (right-hand side scale, in blue) of the OEASTIG cycle as a function of the OEA quality (Ω_{OEA}). Comparison with reference cost of CO_2 capture (reference value of the post-combustion capture process by MEA (monoethanolamine)-absorption.

As shown in Figure 2, the CO_2 capture process decreases the thermal efficiency from 49.4% (efficiency, $\eta_{ref,}$ of the reference power plant (STIG)) to values lower than 43.8% (η_{capt}). The maximum efficiency 43.8% was obtained for Ω_{OEA} close to 0.5 (50% O_2, 50% N_2). For lower Ω_{OEA}, the efficiency decrease is due to the increase in membrane capture cost (from Ω_{OEA}= 0.5 to 0.4, the membrane pressure changes from 1.4 to 3.3 MPa).

For higher Ω_{OEA}, the efficiency decreases because of the increase in the OEA cost (from Ω_{OEA}=0.5 to 0.65, the OEA cost increases from 0.31 to 0.48 kJ/kg$_{O2}$) [3].
Nevertheless, in the Ω_{OEA} range [0.45 - 0.6], the CO_2 capture cost of the OEASTIG cycle is always below 2.5 MJ$_{primary}$/kg$_{CO2}$, the reference value of the post-combustion capture process by MEA(monoethanolamine)-absorption [24][25]. The minimum CO_2 capture cost and the maximum CO_2 avoided were obtained for Ω_{OEA} = 0.5. They are respectively 2.3 MJ$_{primary}$/kg$_{CO2}$ and 0.0983 kg$_{CO2}$/MJ$_{elec.}$
However, this new design leads to substantial modifications in the design of the power plant, especially in the Brayton cycle since the air compressor has to be replaced by a smaller one for OEA feeding, and a compressor as well as a cooler need to be added for the EGR. The characteristics of the cycle elements are reported in Table 1.

	Characteristics of cycle elements							
	P (MPa)	η_{cycle} (%)	C_{fuel} (kg/s)	C_{OEA} (kg/s)	C_{EGR} (kg/s)	T_{urbine} (kg/s)	S_{Steam} (kg/s)	T_{Steam} (K)
STIG (reference)	1.7	49.4	16	573 (air)	0	727	138	828
OEASTIG	1.7	43.8	16	119	438	726	154	873

Table 1: Mass flow meter of each fluid encountered in the power plant. Comparison between the STIG reference cycle and the OEASTIG cycle. η_{cycle}: cycle efficiency, C_{fuel}: fuel flow, C_{OEA}: oxygen enriched flow, C_{EGR}: EGR flow, T_{urbine}: Turbine flow, S_{Steam}: Steam flow, and T_{Steam}: Steam temperature.

1.3. Impact on combustion process

For the studied cycle, the composition of the global mixtures in the combustion chamber as a function of Ω_{OEA} was calculated with EES and is reported in Figure 3.

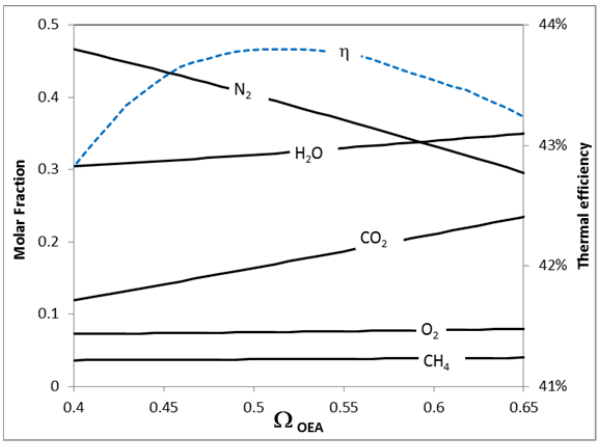

Figure 3: Evolution of the global reactive mixture as a function of OEA quality leading to TIT=1473K.

The composition of the optimum global mixture, obtained for Ω_{OEA}=0.5 corresponding to the maximum thermal efficiency, is reported in table 2. It is compared with the global mixture obtained in AIR/STIG combustion.

Studied Cases				Mixture Mole Fraction				
		β	Ω	X_{N2}	X_{CO2}	X_{H2O}	X_{O2}	X_{CH4}
Air STIG	Global	100%	0.21	55%	0.0%	26.9%	14.5%	3.5%
OEA STIG Ω_{OEA}=0.5	Global	100%	0.16	40.0%	16.6%	32.1%	7.5%	3.75%
	Combustion zone 2073K	38%	0.27	40.2%	12.5%	24.6%	15.2%	7.6%
	combustion zone 2273K	28%	0.31	40.2%	11.0%	21.7%	18.1%	9.0%

Table 2: Compositions of the reactive mixtures in the combustion chamber of AIR/STIG (ϕ= 0.48 and Ω_{OEA}=0.21) and OEASTIG (ϕ = 1 and Ω_{OEA}=0.5). Composition of the global mixture and of the combustion zone leading to flame temperatures (2073 and 2273K). β is the fraction of diluent entering the combustion zone.

As shown in table 2, the new reactive mixtures obtained in OEASTIG have a lower O_2 concentration (X_{O2}) compared to Air/STIG, respectively: X_{O2}=7.5% and 14.5%, due especially to stoichiometric operating conditions. Due to the use of OEA, the mole fraction of N_2 decreases from 55% (in AirSTIG) to 40% (in OEASTIG) and is replaced by H_2O and CO_2. In both OEASTIG conditions, the H_2O mole fraction is double the CO_2 mole fraction: X_{H2O}=32.1% and X_{CO2}=16.6%.
Obviously, this highly H_2O and CO_2 global diluted mixture is not flammable. To obtain a stabilized flame it is necessary to classically split the combustion chamber in two parts: a combustion zone and a dilution zone [4] by distributing the EGR and Steam along the combustion chamber. However, unlike classical GT combustion chambers, all the oxidant (OEA) has to be injected in the combustion zone alone. The scheme of this combustion chamber and its flow distribution are shown in figure 4.

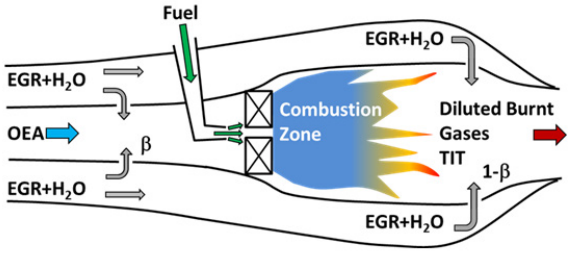

Figure 4: Scheme of the distribution of Fuel, OEA and diluting gases (EGR and H_2O) in the OEASTIG combustion chamber.

Due to the high temperature reached in the combustion zone, a high value of NOx can be expected. To decrease NOx emissions, it would be interesting to operate close to premixed conditions. To keep the same flame structure and stability

without changing the burner design, it is necessary to control the flame temperature and the flame velocity in the combustion zone by adjusting the diluent fraction β fed in this zone (see figure 4). As shown by [6][23], the flame velocity can be linked in a first approximation to the adiabatic flame temperature. Moreover, Taupin et al. [26] showed that a pressurized methane/air swirled flame had a stability domain between ϕ=0.78 (Stable flame, T_{ad}≈2273K) and ϕ=0.65 (Unstable flame close to blow off, T_{ad}≈2073K). Based on these hypotheses and from this temperature range, we chose a β dilution range [β_{min}=28%, β_{max}=38%] of the diluent fraction (table 2) feeding the combustion zone that could lead to a low NOx and stable flame. To show the advantage of H_2O dilution compared to CO_2 dilution, calculated flame velocities and pollutant axial profiles will be presented in the third part of the paper for OEASTIG conditions (pressure and temperature).

2) VALIDATION OF THE REACTION MECHANISM

2.1. Experimental setup

The experiments were made using a stainless steel spherical combustion chamber with an inner diameter of 200 mm for a total volume of 4.2 L. Two opposite and transparent windows (diameter 82 mm) provided optical access to the chamber. The heating of the chamber up to 473 K was controlled by a resistance wire that surrounds the walls of the vessel. Before each gas injection into the chamber, a vacuum was created. The gas volume ($CH_4/N_2/O_2/H_2O$) was controlled and introduced by a mass flow meter (Brooks 5850S, 2 NL/min for N_2, 1.2 NL/min for O_2, and 0.5NL/min for CO_2). For water vapor, a Coriolis mass flow meter (Bronkhorst mini CORIFLOW 30 g/h) was used to convey the water liquid. The inlet valve of water and the mixture were preheated to 473K to ensure water vaporization in the chamber. A perfectly homogenous premixed mixture was obtained by a fan installed inside the chamber. The fan was stopped 5s before each ignition to avoid any perturbation in the mixture. A piezoelectric pressure transducer and a type-K thermocouple were used to check, respectively, the pressure level and the initial temperature before ignition. The maximum deviation between the effective initial pressure inside the combustion chamber and the required initial pressure was about 3%. The temperature fluctuation of the prepared mixture was within 2 K for the target initial temperature. Two tungsten electrodes (diameter of 1mm), with a 1-mm gap, linked to a conventional capacitive discharge ignition system, were used for spark production at the center of the chamber. A LED illuminator (HardSoft DLR IL104G) was used to provide continuous and incoherent light with a wavelength of 528 nm. Parallel light was created using a pinhole of 1 mm diameter and a parabolic mirror (f=865 mm). After passing through both windows of the combustion chamber, the beam was focused on a dot (0.5 mm) with a second parabolic mirror (f=865 mm) and a lens (f=25 mm) re-parallelized the beam directly on the CMOS camera (Phantom V1610) operating from 6000 to 25,000 frames per second, depending on the flame speed expansion and therefore on the oxygen concentration, with an exposure time of 40 µs and a 512x512 pixels frame. Measurements were limited to flames with diameters of 50 mm, corresponding to a volume of burned gases less than 1.6% of the chamber volume. Under this condition, the total chamber pressure can be considered constant during the initial stage of flame expansion.

The temporal evolution of the expanding spherical flame was then analyzed and coupled to the non-linear methodology [27], [28]. This methodology is based on the nonlinear equation proposed by Kelley et al. [29]:

$$\left(\frac{S_b}{S_b^0}\right) 2ln\left(\frac{S_b}{S_b^0}\right) = -\frac{L_b K}{S_b^0} \qquad \text{(Eq.3)}$$

The stretch rate (K), Eq. (4), is defined as the temporal rate of change of a flame surface element of area A:

$$K = \frac{1}{A}\frac{dA}{dt} \qquad \text{(Eq. 4)}$$

In the case of a spherically expanding laminar flame, the total stretch acting on the flame is defined as Eq. (5):

$$K = \frac{2}{R_f}\frac{dR_f}{dt} \qquad \text{(Eq. 5)}$$

Figure 5 shows the experimental measurements (diamonds) of the stretched flame speed (S_b) as a function of the flame stretch (K) for two reactive mixture conditions. The solid line represents the linear correlation, and the dashed line represents the non-linear correlation from which the unstretched propagation flame velocity S_b^0 is extrapolated for K=0.

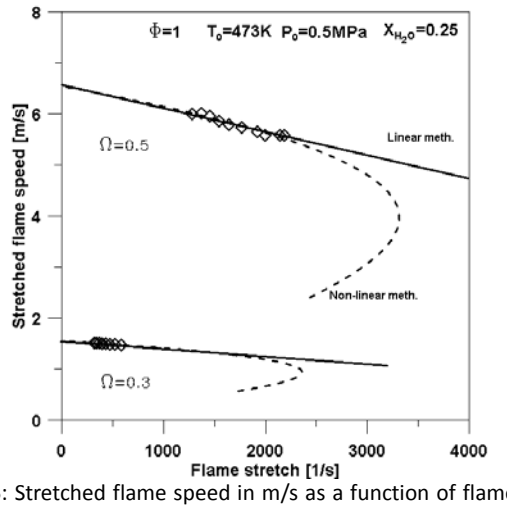

Figure 5: Stretched flame speed in m/s as a function of flame stretch (in s^{-1}) for Ω=0.3 and 0.5, ϕ=1, X_{H2O}=0.25 and P=0.5MPa. Symbol: experimental velocity as a function of flame stretch, dashed line: non-linear methodology, solid line: linear extrapolation methodology.

In the experimental conditions shown in Figure 5, one can observe that the linear methodology (solid line) and non-linear methodology give the same result for S_b^0. This can be explained, as shown in table 3, by low values of the Markstein length whatever the air enrichment (Ω) which involves the non-dependency of the mixture on stretch. The real benefit of the non-linear equation is only observed when the Markstein length

reaches or exceeds 1 mm principally under fuel-lean conditions when the Lewis is higher than the unity.

	H_2O mole fraction	Markstein length	Unstretched propagation flame speed
Ω	X_{H2O}	L_b [m]	S_b^0 [m/s]
0.3	0.25	0.0001896	1.62
0.5	0.25	0.0001283	6.49
0.7	0.65	0.0008565	0.611
1.0	0.65	0.0006005	0.697

Table 3. Markstein length value (L_b) for each condition studied. ϕ = 1, P = 0.5MPa.

The fundamental laminar burning velocity S_L^0 is finally obtained by taking into account the effects of the expansion factor:

$$\frac{s_b^0}{s_L^0} = \frac{\rho_u}{\rho_b} \qquad \text{(Eq.6)}$$

where ρ_u and ρ_b are respectively the density ratios of unburned and burned gases. Assuming kinetic equilibrium, this ratio was estimated thanks to CWB coupled with GRIMech3.0 in isobaric and adiabatic conditions. The ratio ρ_b/ρ_u is presented in figure 6 as a function of water mole fraction, for 0.1 and 0.5MPa, and for Ω=0.21 and 0.5.

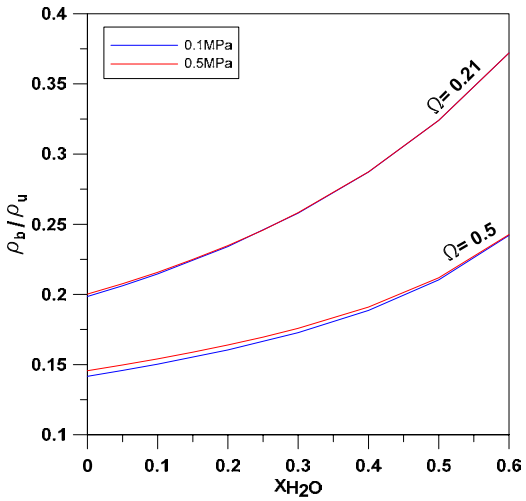

Figure 6: Evolution of the calculated ratio ρ_b/ρ_u (burned and unburned density) as a function of the mole fraction of water, X_{H2O}, for Ω = 0.21 and 0.5 and for P = 0.1MPa (black line) and 0.5MPa (red line). The initial temperature is T_0=473 K, and the equivalence ratio is 1.

2.2. Numerical setup

Simulations of unstretched laminar flame velocities were performed with the Chemical Workbench software package [18] and the GRIMech3.0 mechanism [17]. This code allows the calculation of flame velocity, temperature profiles and species mole fraction profiles in premixed laminar flames by solving for steady, isobaric and 1-dimensional flame propagation equations for continuity, energy, species and state. The present calculations were performed for freely propagating flames including multicomponent and thermal diffusion effects. The flame model uses a high-order spatial discretization scheme and an adaptive mesh. It is important to note that a comparison between CWB and the PREMIX [30] code was carried out (not presented here). The same result was obtained with both softwares using the adaptive mesh parameters GRAD and CURV reduced to 0.001. The density of burnt ρ_b and unburnt ρ_u gases required by the experimental analysis (see equation 6) as well as adiabatic flame temperatures were also computed thanks to CWB (Equilibrium) coupled with GRIMech3.0 in isobaric and adiabatic conditions.

2.4. Comparison between experimental and numerical laminar flame velocities

The unstretched laminar flame velocities were measured for: Ω=0.21 and Ω =0.5, an inlet temperature T_0=473K, and two pressures P = 0.1 and 0.5 MPa. The comparison between experiments and calculations carried out by CWB is presented in Figure 7 as a function of water dilution.

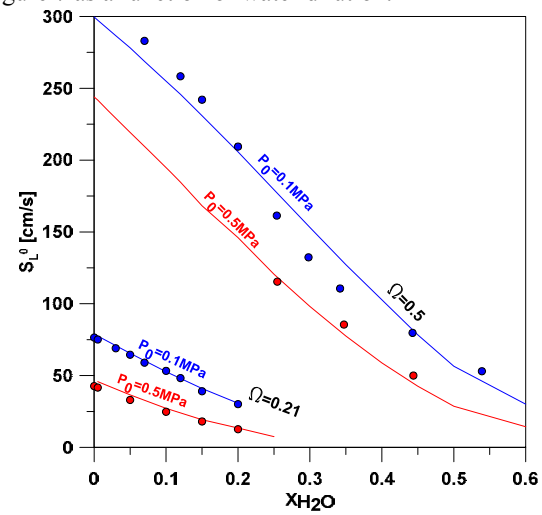

Figure 7: Comparison between experimental (dots) and calculated (lines) unstretched laminar flame velocities as a function of water dilution for T_0=473K and ϕ=1, for 0.1MPa (blue line) and 0.5 MPa (red line) for two conditions of oxygen enrichment Ω=0.21 and 0.5.

As expected, whatever the pressure, 0.1 or 0.5 MPa, and the oxygen enrichment, Ω, experimental and calculated laminar flame velocities decrease when H_2O dilution, X_{H2O}, increases. For a given H_2O dilution and a given Ω, the flame velocity decreases with pressure. For a given pressure and H_2O dilution, laminar flame velocity increases with Ω.

A good agreement is observed between experimental and calculated values, even if the experimental values are always slightly higher than those of the simulations. These results validate the GRIMech3.0 mechanism in this domain of oxygen enrichment and H_2O dilution, demonstrating its reliability for

calculations at higher pressure and temperature conditions that cannot be achieved in a laboratory experimental set-up.
As mentioned above, the laminar flame velocity is a criterion used to predict the flame structure. To maintain the laminar flame velocity constant at e.g. 58 $cm.s^{-1}$ and 0.1 MPa when Ω increases, Figure 7 shows that the X_{H2O} dilution has to be increased from 0.075 (for Ω =0.21) to 0.5 (for Ω =0.5). In the combustion chamber, the flame has to be compact and stable. Moreover, in the case of premixed flame, the flame velocity is a good criterion to predict flashback phenomena.
Temperature and flame velocity are two important criteria for dimensioning the combustion chamber. In a gas turbine, the higher the temperature at the turbine Inlet, the greater the thermal efficiency. But this advantage is limited by the thermal limit of the turbine materials. It is therefore crucial to control this combustion temperature by adjusting the oxidant and dilution flows to prevent turbine damage. As expected and as shown in figure 8, the flame temperature increases as the water dilution decreases and as the air enrichment Ω increases. Moreover the increase in pressure also increases the flame temperature by reducing thermal dissociation.

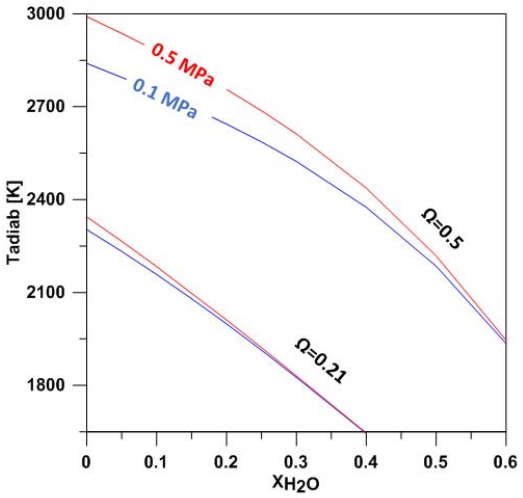

Figure 8: Evolution of the calculated adiabatic flame temperature as a function of water dilution. f=1, T_0=473K, for two pressures P=0.1 and 0.5 MPa and two air enrichments (Ω = 0.21 and Ω=0.5)

3) EXTRAPOLATION IN GAS TURBINE CONDITIONS

3.1. Methodology

In the previous section, it was shown that the reaction mechanism was able to satisfactorily predict flame velocities in a large range of pressure, from 0.1 MPa to 0.5 MPa, Ω, for 21% and 50% and X_{H2O}, from 0 to 0.6 in the initial mixture. Thus, GRIMech3.0 together with CWB was used to extrapolate the calculations of flame velocities in gas turbine conditions.

Our aim was to determine what the inlet compositions compatible with the gas turbine are. In order to answer this question, the study was done in two steps:
-1st step: determination of the initial state leading to the final state described by figure 4 (shown in section 1), i.e. a pressure of 1.7MPa and an adiabatic flame temperature of 2273K (or 2073 K) in the reactive zone (this flame temperature is compatible with the current design of the combustion chamber (see section 1)). The initial state was determined by iterative thermodynamic calculations carried out with CWB and GRIMech3.0 in adiabatic and isobaric (1.7 MPa) conditions, in which H_2O and/or CO_2 dilution, for a given Ω, was the adjustable parameter, for an inlet temperature of 700K and an equivalence ratio set at 1 $\left(\frac{X_{O_2}}{X_{CH_4}} = 2\right)$.
-2nd step: Calculation of the flame velocity corresponding to the initial mixture established in section 1 and determination of the feasible conditions for a gas turbine, i.e. a laminar flame velocity greater than 10 $cm.s^{-1}$ in order to ensure flame stabilization.

3.2. Results

Table 4 shows the results of the 1st step of the methodology described above.

Ω	100	90	70	60	50	40	30	25	21
a) T=2073 K, T_0=700K, P=1.7MPa, ϕ=1									
X_{CO2}	71%	69%	64%	60%	55%	48%	37%	30%	22%
X_{H2O}	76%	74%	69%	66%	61%	54%	43%	35%	26%
b) T=2273 K, T_0=700K, P=1.7MPa, ϕ=1									
X_{CO2}	65%	63%	57%	53%	47%	40%	28%	20%	11%
X_{H2O}	71%	69%	63%	59%	54%	46%	33%	24%	14%

Table 4: Initial composition of the reaction mixture (in terms of Ω and X_{CO2} or X_{H2O}) leading to an adiabatic flame temperature of: a) 2073 K ; b) 2273K.

As shown in table 4, for the same Ω, less carbon dioxide dilution than water dilution is required to reach an identical adiabatic temperature. For instance, in air conditions (i.e. Ω=0.21), a CO_2 mole fraction of 11 % is required whereas a H_2O mole fraction of 14 % is needed to reach an adiabatic temperature of 2273 K. As expected, the higher Ω is, the greater the dilution required to maintain the adiabatic temperature. For CO_2 dilution and an adiabatic temperature of respectively 2073 K and 2273K, it varies from respectively 22% and 11% in air conditions (Ω=0.21) to respectively 71% and 65% in oxycombustion conditions (Ω = 1). For H_2O dilution and an adiabatic temperature of respectively 2073 K and 2273K, it varies from respectively 26% and 14% in air conditions to respectively 76% and 71% in oxycombustion conditions.

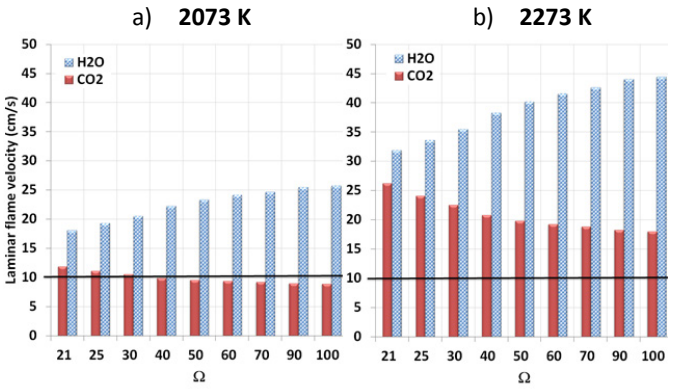

Figure 9: Calculated flame velocities, as a function of Ω, i.e. for the conditions listed in table 4 : a) for T=2073K; b) for T=2273K. The case with H_2O as diluent is shown in blue and that with CO_2 as diluent in red.

Figure 9 shows the flame velocities computed for each initial mixture listed in table 3. As shown in figure 9, the feasible conditions regarding flame stability (i.e. corresponding to a flame velocity greater than 10 $cm.s^{-1}$) are those above the black line. In the case of H_2O dilution, all the conditions are met for 2073K and 2273K. In the case of CO_2 dilution, all the conditions are satisfactory for 2273 K, and for 2073K only the conditions corresponding to the smallest Ω, i.e. for Ω =21%, 25 and 30% can be retained. Figure 9 also shows that, when Ω increases the flame velocity increases in the case of H_2O dilution, whereas it decreases in the case of CO_2 dilution.

In order to understand the effect of H_2O and CO_2 on pollutant emission, it is possible to plot NO and CO mole fractions computed with CWB together with GRIMech3.0 in a freely propagating flame as a function of the distance from the burner In this option, the energy equation is solved assuming an adiabatic system; the value obtained for the highest distance corresponds to thermodynamic equilibrium. The results cannot be compared with what really happens in a gas turbine, but it elucidates the effect of each diluent in a laminar premixed flame. Figure 10 shows the CO and NO mole fraction profiles obtained for Ω=0.21, 0.5 (initial composition listed in table 4) for the two adiabatic temperatures: 2073 and 2273 K.

As expected [31], Figure 10a clearly shows that whatever the adiabatic temperature, an increase in CO_2 dilution and Ω enrichment (dashed lines) leads to an increase in the maximum CO peak mole fraction.

For H_2O dilution (solid lines), the overall effect is the same, but CO production is about half that with CO_2 dilution. This confirms that H_2O dilution is beneficial for CO emission. Obviously, the higher the adiabatic temperature, the higher the CO peak mole fraction is, whatever the diluent. Figure 10b shows the evolution of the NO mole fraction in the flame, i.e. as a function of the distance from the burner. Whatever the conditions, figure 10b clearly shows that H_2O dilution leads to a smaller amount of NO compared to CO_2 dilution. Obviously, no NO is formed when Ω=1 because there is no nitrogen in the initial mixture. A decrease in the flame temperature clearly leads to a decrease in the NO mole fraction. It can be noticed that in the burned gases, the NO mole fraction continues to drastically increase as a function of the distance from the burner, especially for high temperature. In a real flame this drawback can be reduced by decreasing the residence time in hot gases (e.g. by cooling).

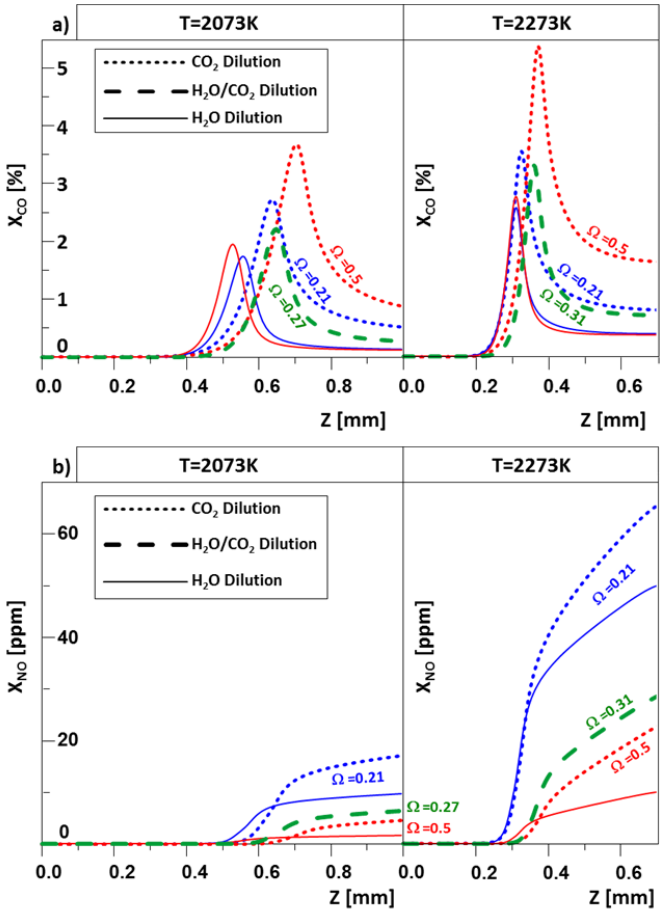

Figure 10: Pollutant Mole fraction as a function of the distance from the burner of: a) CO and b) NO; for T=2073 K and T=2273 K; for: Ω=0.21 (in blue); Ω =0.5 (in red). The case with CO_2 as diluent is represented by dashed lines. The case with H_2O as diluent is represented by solid lines. The green bold dashed lines correspond to the OEASTIG dilution condition (H_2O/CO_2)

In the case of OEASTIG combustion, both H_2O and CO_2 dilution have to be taken into account. Calculations of both flame structure and flame velocities for the two limits (β_{min} and β_{max}) established in table 2 were therefore performed. They lead to S_L^0 = 16.2 cm/s and 30.3cm/s respectively for β =28% (2273 K, Ω=0.27) and 38% (2073K, Ω=0.31). It can be observed that these conditions are compatible with the operation of a gas

turbine from a flame stability point of view, since the flame velocity is greater than 10 cm/s.
On figure 10, we have superimposed (green dashed line) the calculated CO and NO axial profiles for the two OEASTIG conditions corresponding to the β_{min} and β_{max} dilutions in the combustion zone. As the dilution mixture is composed of about 2/3 O_2 and 1/3 CO_2 (see section 1), it can be seen that the level of pollutant production falls between the results obtained with pure CO_2 and pure H_2O dilution, showing the advantage, in comparison with CO_2 dilution in "classical oxycombustion", of injecting this new OEASTIG mixture in the combustion in terms of pollutant production, both for CO and for NO. To further increase this environmental benefit, we could optimize the dilution strategy in the combustion chamber by feeding the combustion zone with the H_2O stream only and the dilution zone with the rest of the dilution mixture (EGR) (fig.11).

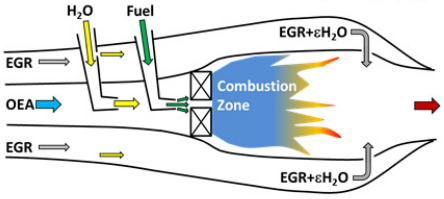

Figure 11: Scheme of the optimized distribution of H_2O and EGR in the OEASTIG combustion chamber.

To simulate the pollutant emissions of these turbulent diluting flames more accurately, it is necessary to use a more appropriate numerical tool as a reactor network [4]. This reactor network will be split in different reaction zones in which the combustion mode and the residence time will be better respected. This is what we plan in the next steps of our study along with an experimental study performed in a pressurized and diluted swirled reference flame.

CONCLUSION

In this study, an innovative thermal cycle based on STIG was proposed. In this cycle, H_2O can be used as an additional dilution flow. The CO_2 capture feasibility of a thermal cycle including the STIG cycle, EGR and OEA coupled with a CO_2 Membrane Separator Unit called OEASTIG was presented and the thermal efficiency of the cycle and especially its impact on the combustion process was studied. It was shown that this new design involves major modifications in the Brayton cycle since the air compressor has to be replaced with a smaller one for OEA feeding, and a compressor and a cooler need to be added for the EGR. Moreover, the use of EGR and steam injection and OEA is certainly going to require modifications in the design of the combustion chamber in order to maintain flame stability and low pollutant emissions. It was also demonstrated that the dilution of the reactive mixture with CO_2 or H_2O and its enrichment with OEA have an impact on the flame structure (shape, length), on its stability and on its pollutant emissions.

The validation of GRIMech3.0 was carried out thanks to experimental and numerical studies. For that purpose, laminar flame velocities of $CH_4/O_2/N_2/H_2O$ mixtures were measured using the shadowgraphy technique in a spherical combustion chamber at atmospheric pressure and high pressure (0.5 MPa) for preheated gas mixtures (T_0=473 K). The ratio $\Omega=X_{O2}/(X_{O2}+X_{N2})$ was varied from 21% to 50% and the mole fraction of H_2O in the mixture was varied from 0 to 80%, for an equivalence ratio of 1. Experimental results were satisfactorily compared with calculations obtained using CWB in conjunction with the GRIMech3.0 mechanism. This study was then extended and numerical simulations were performed at a constant adiabatic temperature, close to the operating temperature of gas turbines.
The present study is a preliminary investigation as the final aim of our work is to compare NO and CO emissions predicted by a gas turbine network coupled with a detailed reaction mechanism to measurements carried out in a reference gas turbine. Thanks to the present work the gas turbine conditions were determined and the reaction mechanism was validated. Furthermore, this preliminary study is of great interest from a combustion point of view because:
- It contributes to the extension of the experimental database on $CH_4/O_2/N_2/H_2O$ laminar flame velocities at high pressure in air and oxygen-enriched conditions.
-It elucidates the effect of H_2O dilution and oxygen enrichment on the flame behavior.

ACKNOWLEDGMENTS

The research leading to these results has received funding from the COCC program in France through the support of the EMC3 Labex and Caprysses Labex.

REFERENCES

[1] B. Belaissaoui, G. Cabot, M. S. Cabot, D. Willson, E. Favre, Chemical Engineering Science 97 (2013) 256–263, CO2 capture for gas turbines: an integrated energy-efficient process combining combustion in oxygen-enriched air, flue gas recirculation, and membrane separation.
[2] Favre E, Roizard D, Bounaceur R, Koros WJ., Ind Eng Chem, Res 2009; 48(7):3700-3701, CO2/N2 Reverse selective gas separation membranes: technological opportunities and scientific challenges.
[3] G. Göttlicher, US Department of Energy, National Energy Technology Laboratory, 2004, The energetics of carbon dioxide capture in power plants.
[4] S.Sundkvist, A. Dahlquist, J. Janczewski, M. Sjödin, M Bysveen, M. Ditaranto, O. Lanngorgen, M. Seljeskog, M. Siljan, Journal of engineering for gas turbines and power, Oct 2014, vol. 136 - 101513, Concept for a combustion in oxyfuel gas turbine combined cycles.
[5] I. Saanum, M. Ditaranto, A. Schonborn, J Janczewski, Proceedings of ASME Turbo Expo, GT2016-57142,

Demonstration plant and combustion system for an oxy-fuel gas turbine.
[6] Lafay, Y.; Taupin, B.; Martins, G.; Cabot, G.; Renou, B.; Boukhalfa, A. Exp. Fluids 2007, 43 (2−3), 395−410, Experimental study of biogas combustion using a gas turbine configuration.
[7] S. de Persis, G. Cabot, L. Pillier, I. Gökalp, A. M. Boukhalfa, Energy & Fuels 2013, 27, 1093−1103, Study of Lean Premixed Methane Combustion with CO2 Dilution under Gas Turbine Conditions.
[8] LeCong T and Dagaut P. Experimental and Detailed Kinetic Modeling of the Oxidation of Methane and Methane/Syngas Mixtures and Effect of Carbon Dioxide Addition. Combust SciTechnol 2008;180: 2046-91.
[9] S. de Persis, F. Foucher, L. Pillier, V. Osorio, I. Gökalp, Energy 55 (2013), pp.1055-66, Effects of O2 enrichment and CO2 dilution on laminar methane flames.
[10] Konnov AA, Dyakov IV. Measurement of propagation speeds in adiabatic cellular premixed flames of CH4 + O2 + CO2. Experimental Thermal and Fluid Science 2005;29(8):901e7.
[11] D. X. Du, R. L. Axelbaum, C. K. Law. The influence of carbon dioxide and oxygen as additives on soot formation in diffusion flames. Twenty-Third Symposium (International) on Combustion/The Combustion Institute, 1990/pp. 1501-1507.
[12] Heil, P.; Toporov, D.; Förster, M.; Kneer, R. Experimental investigation on the effect of O2 and CO2 on burning rates during oxyfuel combustion of methane. Proc. Combust. Inst. 2011, 33 (2), 3407−3413.
[13] Albin E, Nawroth H, Göke S, D'Angelo Y, Paschereit C.O, Experimental investigation of burning velocities of ultra-wet methane–air–steam mixtures, Fuel Processing Technology 107 (2013) 27–35.
[14] Mazas, A.; Fiorina, B.; Lacoste, D.; Schuller, T. Effects of water vapor addition on the laminar burning velocity of oxygen–enriched methane flames. Comb. and Flame 2009. 158 (2011) 2428-2440.
[15] B. Galmiche, F. Halter, F. Foucher, P. Dagaut, Effects of dilution on laminar burning velocity of premixed methane/airflames, Energy & Fuels 25 (3) (2011) 948–954.
[16] V.S. Babkin, A.V. V'yun, Fiz. Goreniya Vzryva. Effect of water vapor on the normal burning velocity of a methane/air mixture at high pressure.7 (3) (1971) 392–395.
[17] G. Smith, D. Golden, M. Frenklach, N. Moriarty, B. Eiteneer, M. Goldenberg, C. Bowman, R. Hanson, S. Song, W. Gardiner, V. Lissianski, and Z. Qin; "GRI-Mech 3.0" [online]; http://www.me.berkeley.edu/gri_mech/
[18] CWB, Deminsky, M., Chorkov, V., Belov, G., Cheshigin, I., Knizhnik, A., Shulakova, E., Shulakov, M., Iskan-darova, I., Alexandrov, V., Petrusev, A., Kirillov, I.,Strelkova, M., Umanski, S., and Potapkin, B., Comput. Mater. Sci. , 2003, vol. 28, p. 169.
[19] Klein KA, Alvarado FL. EES Engineering Equation Solver, version 8.600 ND. Middleton: F-Chart Software; 2004.
[20] B. Belaissaoui , G. Cabot, M.S. Cabot, D. Willson, E. Favre, Energy 38 (2012) 167-17,5 An energetic analysis of CO2 capture on a gas turbine combining flue gas recirculation and membrane separation.
[21] Lefebvre AH., ISBN 1-56032-673-5, 1999 Gas turbine combustion. Taylor & Francis.
[22] DG. Jandjel, 2000; 96(7):15-29., Chem Eng Prog, Select the right compressor.
[23] G. Cabot, M. Calbry, P. Xavier, A. Vandel, S. de Persis, L. Pillier, B. Belaissaoui, E. Favre, Proceedings of ASME Turbo Expo, GT2014.25781, Effect of CO2 capture on combined cycle gas turbine efficiency using membrane separation, EGR and OEA effects on combustion characteristics.
[24] Lars Erik Øi, SIMS2007 Conference, Gøteborg, October 30-31st 2007, Aspen HYSYS Simulation of CO2 Removal by Amine Absorption from a Gas Based Power Plant.
[25] Singh D, Croiset E, Douglas PL, Douglas MA., Energy Convers Manage 2003; 44:3073, Techno-economic study of CO2 capture from an existing coal-fired power plant: MEA scrubbing vs O2/CO2 recycle combustion.
[26] B. Taupin, G. Cabot, G. Martins, D. Vauchelles, A. Boukhalfa. Comb. Sc. And Tech., 179: 117-136, 2007, Experimental Study of Stability, Structure and CH Chemiluminescence in a Pressurized Lean Premixed Methane Turbulent Flame.
[27] Tahtouh T, Halter F, Mounaïm-Rousselle C. Measurement of laminar burning speeds and Markstein lengths using a novel methodology. Combustion and Flame 2009; 156:1735e43.
[28] D. Bradley, R.A. Hicks, M. Laws, C.G.W. Sheppard, Combustion and Flame 1998; 115-539-50, The measurement of laminar burning velocities and Markstein numbers for iso-octane-air and iso-octane-n-heptane-air mixtures at elevated temperatures and pressures in an explosion bomb.
[29] Kelley, A. P.; Law, C. K. Nonlinear effects in the extraction of laminar flame speeds from expanding spherical flames. Combust. Flame 2009, 156, 1844–1851.
[30] Kee, R. J.; Rupley F. M. and Miller J. A.; Sandia Report SAND89-8009B; 1989; Chemkin-II: A Fortran Chemical Kinetics Package for the Analysis of Gas Phase Chemical Kinetic.
[31] A. Amato et al., Methane Oxy-Combustion for low CO2 Cycles: Measurement and modeling of CO and O2 emissions, Proceedings of ASME Turbo Expo GT 2010-22300.